Substrate Binding Mechanism of Glu180→Gln, Asp176→Asn, and Wild-Type Glucoamylases from *Aspergillus niger*†

Ulla Christensen,*,‡ Karsten Olsen,‡ Bjarne B. Stoffer,‡ and Birte Svensson§

Chemical Laboratory IV, University of Copenhagen, DK-2100 Denmark, and Department of Chemistry, Carlsberg Laboratory, DK-2500 Denmark

Received April 8, 1996; Revised Manuscript Received September 6, 1996⊗

ABSTRACT: Glucoamylase (1,4-α-glucan glucohydrolase, EC 3.2.1.3) from *Aspergillus*, of which the 3D structure is known, releases β-D-glucose from the non-reducing ends of starch and other related oligo- and polysaccharides, cleaving the α-1,4-bond positioned between subsites 1 and 2 in the enzyme−substrate complex. The presteady and steady state kinetics of two of the existing mutants, Glu180→Gln and Asp176→Asn, are presented here. The kinetic results are analyzed according to two reaction models: One suggested previously [Olsen, K., Svensson, B., & Christensen, U. (1992) *Eur. J. Biochem. 209*, 777−784], which contains three consecutive steps of the reaction, and one generally accepted and used in calculations of subsite energies [Hiromi, K. (1970) *Biochem. Biophys. Res. Commun. 40*, 1−6], which assumes important non-productive binding and identical values of the intrinsic catalytic constant independent of the chain length of the substrate. It is found that glucoamylase shows kinetics in accordance with a consecutive three-step mechanism, in which the formation of the Michaelis complex occurs in two steps and is followed by a slow catalytic step and fast dissociation of the products with no accumulation of enzyme−product complexes. The kinetics, however, are not in accordance with the model generally used in subsite energy calculations. Thus the kinetic model on which very low values of subsite 1 and high values of subsite 2 interaction energies have been based is not correct. A greater importance of subsite 1 interactions than has hitherto been anticipated is indicated. The results of the Glu180→Gln mutant show weak overall binding, which stems from large effects on the formation of the Michaelis complex in the second step of the reaction, but no or rather small effects on the initial association of enzyme and substrate, except for maltose. The mutant further shows effective catalysis. A hydrogen bond of the side chain carboxylate of Glu180 with the 2-OH of the sugar ring at subsite 2 is an expected important interaction of the Michaelis complex, as seen from the 3D structures of stabile enzyme−inhibitor complexes. Apparently this bond is established in the second reaction step. It is indicated that subsite 1 and 3 interactions to a great extent govern the initial association. In accordance with a dynamic role of Glu180, structural energy minimization calculations show a flexibility of the γ-carboxylate of Glu180. The side chain of Asp176 participates in a hydrogen-bonding network also involving the backbone of Glu180 and Glu179, the catalytic acid. Compared with the wild-type enzyme, the Asp176→Asn mutant shows no significant changes in binding. The catalytic rate is, however, markedly reduced. Apparently changes in the hydrogen bonding network of Asp176 are of importance in the rate-determining catalytic step, but not in the substrate binding steps. Structural energy minimization calculations on the Asp176→Asn mutant, however, do not confirm this assumption.

Glucoamylase (1,4-α-D-glucan glucohydrolase, EC 3.2.1.3) from *Aspergillus*, of which the 3D-structure is known (Aleshin et al., 1992, 1994; Harris et al., 1993; Stoffer et al., 1995), catalyzes the release of β-D-glucose from the non-reducing ends of starch and related oligo- and polysaccharides (Hiromi et al., 1983). Also 1,6-α-D-glucosidic bonds are hydrolyzed, but with much lower efficiency (Hiromi et al., 1966a,b). The glucoamylases from *Aspergillus awamori* var. *X100* and *Aspergillus niger* are practically identical and show identical active site structure (B. B. Stoffer, A. E. Aleshin, M. Gajhede, B. Svensson, and R. B. Honzatko, unpublished). As for other inverting carbohydrases [for a review see Svensson and Søgaard (1993)] two carboxyl groups, Glu179 and Glu400, serve respectively as general acid and general base catalysts in the reaction mechanism (Hiromi et al., 1966a; Svensson et al., 1990; Sierks et al., 1990; Harris et al., 1993; Frandsen et al., 1994). Conserved Trp residues are involved in interactions of the enzymes with substrates and inhibitors (Hiromi et al., 1983; Clarke & Svensson, 1984a,b; Sierks et al., 1989), and changes in the intrinsic enzyme fluorescence result when binding occurs. These changes were earlier assumed to involve only subsite 1 (Hiromi et al., 1983), but recent structure and function studies have shown that this is not correct (Clarke & Svensson, 1984a; Svensson & Sierks, 1992; Aleshin et al.,

† This work was supported by the Danish Technology Council (Grant 1990-133/443-900088), by the Danish Natural Science Research Council [Grants 11-6876 and 11-7542 (U.C.)], by the Carlsberg Foundation [Grants 950248/20 (B.B.S.), 88-0093/40, and 89-0098/10 (U.C.)], and by the Novo Foundation Committee [(1993) (U.C.)].

* Address correspondence to this author at Chemical Laboratory IV, Universitetsparken 5, DK-2100 Copenhagen, Denmark. Tel: +45 35 32 02 66. FAX: +45 35 32 02 99.

‡ University of Copenhagen.

§ Carlsberg Laboratory.

⊗ Abstract published in *Advance ACS Abstracts,* November 1, 1996.

S0006-2960(96)00832-X CCC: $12.00

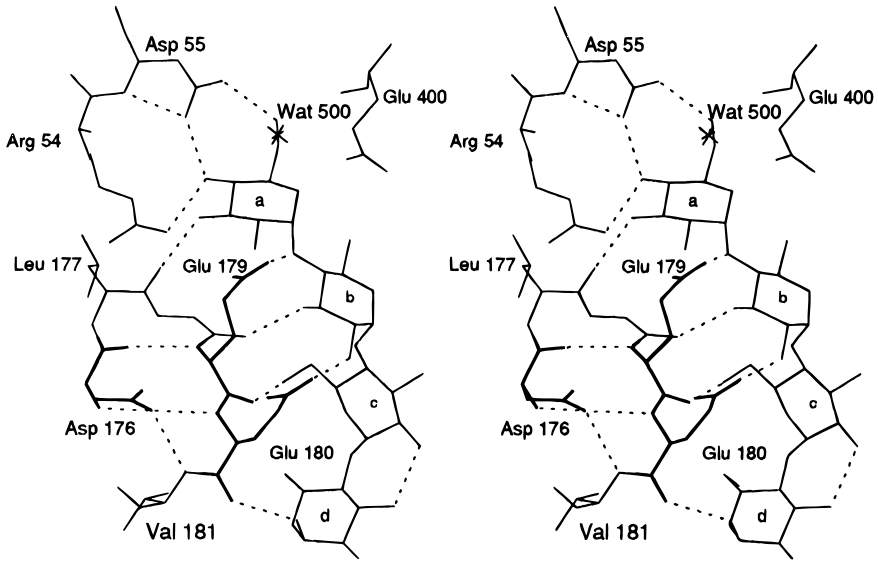

FIGURE 1: Stereoview of the active site of glucoamylase from *A. awamori* var. *X100* with bound D-*gluco*-dihydroacarbose (Stoffer et al., 1995). Asp176 and Glu180 are shown with bold lines, and hydrogen bond interactions less than 3.0 Å are represented by dashed lines. To simplify the view the side chain of Trp178 is not shown.

1992; Sierks et al., 1993; Olsen et al., 1993; Stoffer et al., 1995).

To obtain better a understanding of structure/function relationships of the glucoamylases from *Aspergillus* we have undertaken presteady state kinetic studies of the substrate binding mechanism of the *A. niger* enzyme and mutants hereof (Olsen et al., 1992, 1993). Analysis of the results according to a three-step reaction mechanism (Model I) of substrate catalysis involving two intermediates, ES, the initial association complex, and E*S, the Michaelis complex (i.e., the most stable enzyme−substrate intermediate) (Ohnishi & Hiromi, 1978; Tanaka et al., 1982; Hiromi et al., 1983; Ohnishi, 1990), showed excellent compatibility (Olsen et al., 1992, 1993). But as an important feature of our model, in agreement with the suggestions of Fagerström (1991) and in contrast to other Model I-type suggestions, we argue (Olsen et al., 1993) that subsite 1 is involved in the formation of the ES complex and that the transformation of ES to E*S involves conformational changes and not the filling of a previously empty subsite 1 by relocation of the substrate:

$$E + S \underset{k_{-1}}{\overset{k_1}{\rightleftharpoons}} ES \underset{k_{-2}}{\overset{k_2}{\rightleftharpoons}} E^*S \xrightarrow{k_3} E + P \quad \text{(Model I)}$$

Be that as it may, presteady state kinetics results have never been analyzed with respect to their possible accordance with the classical model (Hiromi, 1970; Hiromi et al., 1973, 1983) of glucoamylase-catalyzed reactions (Model II). This is important because Model II, in spite of its incompatibility with Model I, is being used for subsite energy calculations (Hiromi et al., 1983; Meagher et al., 1989; Sierks et al., 1989; Sierks & Svensson, 1993; Frandsen et al., 1994, 1995; Hiromi, 1995). Model II assumes important non-productive binding of the substrates and substrate length independent values of the intrinsic catalytic constant (k_{+2} in our notation):

$$ES_{NP} \underset{k_{-3}}{\overset{k_{+3}}{\rightleftharpoons}} E + S \underset{k_{-1}}{\overset{k_{+1}}{\rightleftharpoons}} ES \xrightarrow{k_{+2}} E + \text{products} \quad \text{(Model II)}$$

The general acceptance of subsite 2 of glucoamylase as that providing most of the binding energies of substrates is based on Model II. Clearly, it is important to investigate whether we have to condemn or to recognize Model II more fully.

The present study reports presteady and steady state kinetic results on the interactions of the wild-type and the Glu180→Gln and Asp176→Asn mutant glucoamylase G1 from *A. niger* with the maltooligosaccharide series (S_x), maltose (S_2) to maltotetraose (S_4) and focuses on analysis of the data according to Model I as well as Model II, which, respectively, excludes and includes non-productive binding. As seen from the 3D structure of glucoamylase−inhibitor complexes (Aleshin et al., 1994; Stoffer et al., 1995) and as illustrated in Figure 1 the carboxylate function of Glu180 directly interacts with the sugar ring at subsite 2 and is thus expected to be srongly involved in subsite 2 binding of inhibitors. The Glu180→Gln mutant therefore is an excellent tool for gaining better insight into the binding mecahnism, particularly with respect to the assignment of subsite 2. The side chain of Asp176 participates in a hydrogen-bonding network also involving the backbone of Glu180 and Glu179 (Harris et al., 1993; Stoffer et al., 1995) and may play a role in substrate binding, if mobility of this segment is needed.

MATERIALS AND METHODS

Materials. Mutant plasmids harboring inserts encoding Glu180→Gln and Asp176→Asn glucoamylase G1 from *A. niger* were made and used for *A. niger* transformation essentially as described (Sierks et al., 1990; Frandsen et al., 1994). The G1 and G2 forms were purified from the culture liquid by an established protocol involving affinity chromatography on acarbose-Sepharose (Clarke & Svensson, 1984b) and FPLC-chromatography on a High Load Q-Separose (Stoffer et al., 1993). Protein concentration was determined spectrophotometrically at 280 nm using $\epsilon_M = 1.37\ 10^5\ M^{-1}\ cm^{-1}$ (Clark & Svensson, 1984a) as for th wild-type. Maltose and maltotetraose were from Merck (Darmstadt, Germany), and maltotriose was from Aldrich (Steinheim, Germany). The D-glucose oxidase kit for determination of glucose was purchased from Sigma Chemical Co. (St. Louis, MO).

Stopped-Flow Fluorescence Kinetics. The presteady state kinetics of the binding of ligands to the glucoamylase mutants

were followed by measuring the changes of the intrinsic protein fluorescence intensity essentially as described by Olsen et al. (1992, 1993). Experiments were performed in a Hi-Tech Scientific PQ/SF-53 spectrofluorimeter equipped with a high-intensity xenon arc lamp. The excitation wavelength was 280 nm, slit width 5 mm. Light emitted from the reaction mixture was monitored after passage of a cutoff emission filter (WG 320; 80% transmittance at 320 nm). In this way an integrated emission signal is obtained. A series of stopped-flow experiments were performed at 8 °C in 0.05 M acetate buffer, pH 4.5. After rapid mixing of enzyme (Glu180→Gln and Asp176→Asn glucoamylase G1 mutants, final concentrations, respectively, 3.5 and 2.8 μM) and the appropriate ligand solution the time course of the intrinsic fluorescence intensity (Arbitrary units, V) was recorded. Mixing was achieved in less than 1 ms. In each experiment 400 pairs of data were recorded, and generally sets of data from four experiments were averaged. Each averaged set of stopped-flow data was then fitted to a number of nonlinear analytical equations using the Hi-Tech HS-1 Data Pro software. Typical stopped-flow traces of the binding of substrates to these mutants were similar to those obtained previously of wild-type and Trp120→Phe glucoamylase (Olsen et al., 1992, 1993) in showing only one relaxation and best fitted curves corresponding to a single-exponential progress (eq 1):

$$\Delta F([S_x],t) = \Delta F([S_x],\infty)(1 - \exp(-k_{obs}t)) \qquad (1)$$

where k_{obs} (general precision: ±3%) is the observed first-order rate constant, and $\Delta F([S_x],t)$ (general precision: ±1%) is the relative fluorescence change observed at the actual ligand concentration, $[S_x]$, and time, t. The steady state value $\Delta F([S_x],\infty)$ is attained at a time, t, where no (or only negligible) hydrolysis has yet occurred. Equation 1 describes the most accurate fit to the measured data at all concentrations of all ligands employed. The regression analysis used i based on the Gauss−Newton procedure.

Steady State Kinetic Analysis. The hydrolysis of maltooligodextrins was performed in 0.05 M sodium acetate, pH 4.5 at 8 °C using 16 nM Glu180→Gln mutant glucoamylase and eight to ten substrate concentrations in the following ranges: maltose, 1−45 mM; maltotriose, 0.25−15 mM; maltotetraose, 0.5−15 mM; and 0.5 μM Asp176→Asn mutant and maltose 0.1−5 mM. Each initial rate was based on seven to ten points of the progress curve of the reaction. The aliquots removed were quenched and assayed by the glucose oxidase method (Fleming & Pegler, 1963) as previously reported (Olsen et al., 1992).

Structural Analysis. The complex between glucoamylase from *A. awamori* var. *X100* and D-gluco-dihydroacarbose at pH 4 (Stoffer *et al*., 1995) and the software program packages, Insight II and Discover (Biosym Technologies, San Diego, CA), were used for structure analysis and structure energy minimization calculations. In order to mimic a situation with bound substrate in the active site of the enzyme, D-*gluco*-dihydroacarbose was modified into maltotetraose, followed by removal of all disordered residues. By default Discover incorrectly assigns a single bond to the carbonyl function of *N*-acetyl glucosamines in *N*-linked carbohydrate units of the protein. After correction of the bond order of these bonds hydrogen atoms were added to the maltotetraose model complex, selecting a pH value of 4.0, a chapping mode including charges, and the standard forcefield CVFF. When hydrogen atoms are added under these conditions, Insight II suggests Asp176 to be a charged residue, whereas Glu179, Glu180, and Glu400 are suggested to be uncharged. Glu400 was modified to a charged residue by deletion of the hydrogen of the γ-carboxylate group, which brings the maltotetraose model structure to correlate with the charged state of Glu179 and Glu400 as previously suggested (Frandsen et al., 1994). The effect of mutating Asp176 was analyzed by replacing Asp176 by Asn in the original maltotetraose model complex. The position of the side chain amide group of Asn176 was selected in two conformations: the first one with the position of ND2 equal to OD1 of Asp176 and the second one with the position equal to OD2 of Asp176. The two conformations of Asn176 were treated as two separate parallel minimization experiments. Both wild-type and mutated maltotetraose model structures were minimized for 6000 iterations using Discover and the steepest descent algorithm with double-cutoff values for nonbonded interactions set to 20 and 25 Å.

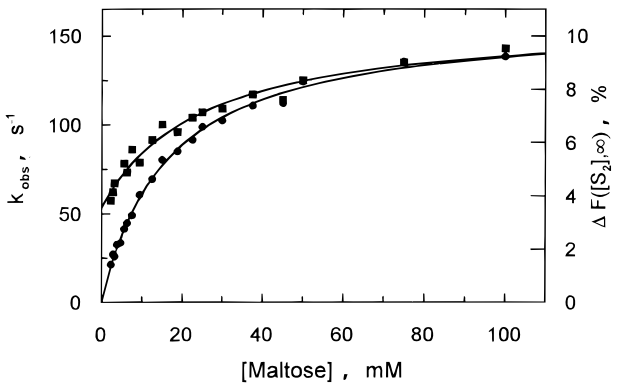

FIGURE 2: Glu180→Gln mutant glucoamylase stopped-flow kinetic results. The example shows the dependencies of the observed rate constant, k_{obs} (filled squares), and of the final change of the fluorescence, $\Delta F([S_2],\infty)$ (filled circles) (eq 1), on the concentration of maltose, the S_2 substrate. The lines shown are those obtained from fitting eq I.3 (and eq II.8) for k_{obs} (or α) and a simple hyperbolic equation for $\Delta F([S_2],\infty)$ to the data. Experimental conditions: pH 4.5, 8 °C, 3.5 μM enzyme. Relative standard deviation: ±3%. The two parameters were in each case determined from a series of time courses of the intrinsic protein fluorescence intensity decrease caused by the binding of the substrate each showing a single-exponential decay. Excitation wavelength was 280 nm. The signal represents the integrated, total fluorescence emission intensity above 320 nm.

RESULTS

Kinetic Analysis. Interactions of glucoamylase and mutants thereof with ligands (e.g., substrates) can be followed in the millisecond time scale using the stopped-flow method of mixing and fluorescence measurement for detection of the reactions (Olsen et al., 1992; 1993). Here the presteady state, as well as the steady state kinetics of two mutants, Glu180→Gln and Asp176→Asn, has been investigated.

As for the wild-type and Trp120→Phe mutant glucoamylases (Olsen et al., 1993), the Glu180→Gln and the Asp176→Asn mutants, in all runs in each series of stopped-flow kinetic experiments performed, showed single-exponential presteady state behavior. The concentration dependences of the two parameters obtained from fits of eq 1 to such data with maltose as the substrate are illustrated in Figures 2 and 3. Similar patterns of concentration depend-

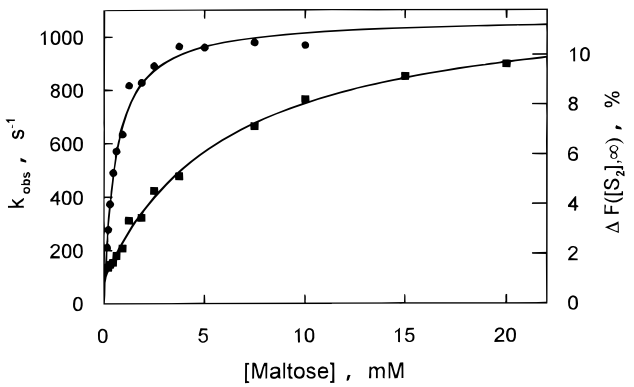

FIGURE 3: Asp176→Asn mutant glucoamylase stopped-flow kinetic results. The example shows the dependencies of the observed rate constant, k_{obs} (filled squares), and of the final change of the fluorescence, $\Delta F([S_2],\infty)$ (filled circles) (eq 1) on the concentration of maltose, the S_2 substrate. The lines shown are those obtained from fitting eq I.3 for k_{obs} and a simple hyperbolic equation for $\Delta F([S_2],\infty)$ to the data. $\Delta F([S_x],\infty)$ values were obtained at reaction times at which no hydrolysis was yet observed. Experimental conditions: pH 4.5, 8 °C, 2.8 μM enzyme. Relative standard deviation: ±3%.

encies were obtained with maltotriose and maltotetraose as substrates (not shown).

Mechanistic Interpretation. A mechanistic interpretation of kinetic results requires that correspondence exists between the observed concentration dependence of a measured kinetic parameter and that predicted by the equations that governs that particular mechanism. As shown previously for the wild type (Olsen et al., 1992, 1993), a mechanistic interpretation of the experimental data shown in Figures 2 and 3 immediately rejects a simple model, as

$$E + S \rightleftarrows E^*S \rightarrow E + P$$

which requires a linear dependent of k_{obs} on the substrate concentration. Figures 2 and 3 clearly show nonlinear dependences of k_{obs} as a function of the substrate concentrations.

Analysis According to Model I. The steady state kinetic parameters of Model I (shown above) are

$$k_c = k_2k_3/(k_2 + k_3 + k_{-2}) \qquad (I.1)$$

and

$$K_m = (k_{-1}(k_2 + k_3) + k_2k_3)/(k_1(k_2 + k_3 + k_{-2})) \qquad (I.2)$$

where K_m and k_c are the regular kinetic parameters of the Michaelis−Menten equation. The presteady state equation of Model I (Olsen et al., 1993), leads to a simple first-order rate expression, eq 1, if the first association is fast compared with the dead time of the stopped-flow instrument (<1 ms). The rate constant k_{obs}, shows a hyperbolic dependence on the concentration of the substrate, [S], from which $K_1 = k_{-1}/k_{+1}$, k_{+2}, and k_{-2} of Model I may be obtained:

$$k_{obs} = k_{+2}/[1 + K_1/(s)] + k_{-2} \qquad (I.3)$$

Further, according to Model I the fluorescence change is proportional to the concentration of E*S at any given time and its final value at concentration $[S_x]$ of the substrate, $\Delta F([S_x],t\rightarrow\infty)$, is a hyperbolic function of $[S_x]$ with a limit value, $\Delta F_{max}(S,\infty)$, which is the maximal relative fluorescence change at saturation with the actual kind of substrate, with a characteristic half-saturation substrate concentration, K_d:

$$K_d = [K_1k_{-2}/k_{+2}]/(1 + k_{-2}/k_{+2}) \qquad (I.4)$$

When the catalytic constant, k_3, is very small compared to k_2 and k_{-2}, one further obtains $K_m = K_d$ (eqs I.2 and I.4).

Tables 1−3 show the results of an analysis according to Model I of the experimental data obtained on the Glu180 and the Asp176 mutants together with some previously obtained on the wild type and Trp120→Phe mutant. All results are in accordance with Model I. The equality of K_d and K_m values obtained from respectively presteady state and steady state kinetic measurements shows that no other intermediates are present in significant amounts, since $K_m = [E][S]/\sum[ES_x]$, where x represents all types of existing enzyme−substrate complexes, and $K_d = [E][S]/([ES] + [E^*S])$. The value of K_m would be significantly less than that of K_d, if steady state concentrations of other intermediates were not insignificant. Also very important to note is the observation that the total fluorescence of the various glucoamylases is equal to that obtained at (the extrapolated) zero time of the reactions. Thus, according to Model I the fast formation of the first [ES] complex does not in any case result in a fluorescence change, which seems more plausible if the complex formd is bound relatively weakly, rather than strongly, e.g., due to strong subsite 2 interaction.

Analysis According to Model II. As outlined above it seems important also to perform an analysis of the results according to Model II.

Model II, in which two kinds of enzyme−substrate complexes are formed in the presteady state phase of the reaction, contains two different, but coupled, association reactions, where in our notation

$$K_i = k_{-3}/k_3 \qquad (II.1)$$

is the inhibition constant of the non-productive binding,

$$K_m = (k_{-1} + k_{+2})/k_{+1} \qquad (II.2)$$

is the inhibition free Michaelis constant of the system, k_{+2} is the intrinsic catalytic constant,

$$k_{cat} = k_{+2}K_i/(K_i + K_m) \qquad (II.3)$$

is the steady state kineic catalytic constant, and

$$K_{m,app} = K_iK_m/(K_i + K_m) \qquad (II.4)$$

is the steady state kinetic Michaelis constant. Presteady state kinetics under pseudo-first-order reaction conditions, necessary for eventually attaining a steady state, would show biexponential behavior with $k_{obs,1} = \beta$ and $k_{obs,2} = \alpha$ ($\beta > \alpha$), as is evaluated in the Appendix, eqs A20 and A19, respectively.

This is never observed. However, association reactions can be too fast for detection in a stopped-flow experiment, where the upper limit of reliable k_{obs} values due to the dead time of the instruments is of the order 10^3 s^{-1}, and k_{obs} values much greater than that would not be determined.

Thus, if the reaction meets the requirement $\beta = k_{obs,1} > 5 \times 10^3$ s^{-1}, Model II, as is the case of Model I, may be compatible with the observation of only a single exponential in the presteady state phase.

Table 1: Results for the Reaction of Maltose with Wild-Type and Mutant Glucoamylases (pH 4.5, 8 °C)

enzyme	K_1 (mM)	k_2 (s^{-1})	k_{-2} (s^{-1})	$\Delta F_{max}(S_x,\infty)$ (%)	K_d (μM)	K_m (μM)	k_c (s^{-1})
Glu180→Gln	25.0 ± 5.5	106 ± 6	54 ± 4	10.7 ± 0.2	(16 ± 0.6) × 10^3	(15 ± 2) × 10^3	0.16 ± 0.05
Asp176→Asn	6.1 ± 0.7	1070 ± 40	90 ± 14	11.5 ± 0.3	600 ± 40	−	−
wild-type[a]	3.4 ± 0.1	1170 ± 10	33 ± 1	19.7 ± 0.2	270 ± 10	180 ± 20	0.33 ± 0.01
Trp120→Phe[a]	5.2 ± 0.5	1150 ± 30	4.3 ± 0.5	17.5 ± 0.4	45 ± 5	52 ± 3	0.01 ± 0.002

[a] Data from Olsen et al. (1993).

Table 2: Results of the Reaction of Maltotriose with Wild-Type and Mutant Glucoamylases (pH 4.5, 8 °C)

enzyme	K_1 (mM)	k_2 (s^{-1})	k_{-2} (s^{-1})	$\Delta F_{max}(S_x,\infty)$ (%)	K_d (μM)	K_m (μM)	k_c (s^{-1})
Glu180→Gln	3.4 ± 1.0	285 ± 25	125 ± 20	7.0 ± 0.5	(5 ± 0.7) × 10^3	(5.6 ± 0.7) × 10^3	1.5 ± 0.05
Asp176→Asn	1.0 ± 0.1	990 ± 45	18 ± 11	10.3 ± 0.3	120 ± 10	−	−
wild-type[a]	2.0 ± 0.1	1630 ± 20	23 ± 1	19.5 ± 0.2	53 ± 2	57 ± 6	1.75 ± 0.05
Trp120→Phe[a]	7.0 ± 0.3	770 ± 15	2.2 ± 0.2	15.5 ± 0.2	20 ± 2	44 ± 5	0.034 ± 0.001

[a] Data from Olsen et al. (1993).

Table 3: Results of the Maltotetraose Reaction with Wild-Type and Mutant Glucoamylases (pH 4.5, 8 °C) in Accordance with Model I

enzyme	K_1 (mM)	k_2 (s^{-1})	k_{-2} (s^{-1})	$\Delta F_{max}(S_x,\infty)$ (%)	K_d (μM)	K_m (μM)	k_c (s^{-1})
Glu180→Gln	2.3 ± 1.1	550 ± 80	270 ± 90	12.7 ± 0.6	(6.4 ± 0.8) × 10^3	(5.1 ± 0.8) × 10^3	2.8 ± 0.3
Asp176→Asn	2.1 ± 0.3	2000 ± 150	∼2	6.7 ± 0.1	30 ± 3	−	−
wild-type[a]	2.5 ± 0.1	2300 ± 70	13 ± 1	17.5 ± 0.2	20 ± 2	32 ± 6	3.2 ± 0.2
Trp120→Phe[a]	4.5 ± 0.3	350 ± 15	0.4 ± 0.04	13.3 ± 0.2	7 ± 0.3	∼30	0.06 ± 0.003

[a] Data from Olsen et al. (1993).

Table 4: Values Resulting from an Analysis of the Reactions of Wild-Type Glucoamylase (pH 4.5, 8 °C) Using Model II

substrate	range of K_m from $K_{1,obs}$ (mM)[a]	α_∞ (s^{-1})	α_0 (s^{-1})	range of $K_{m,app}$ from α_0, α_∞, and $K_{1,obs}$ (mM)[b]	$K_{m,app}$ (mM)	$k_{c,app}$ (s^{-1})	range of resulting k_{+2} value (s^{-1})[c]
maltose	3.4−6.8	1170	33	0.1−0.27	0.18	0.33	6−12
maltotriose	2.0−4.0	1630	23	0.03−0.06	0.06	1.8	58−120
maltotetraose	2.5−5.0	2300	13	0.014−0.03	0.03	3.2	250−500

[a] From eq II.16. [b] From eq II.10. [c] From eq II.18.

The corresponding k_{obs} then is the α of eq A19, given that $\beta > 5 \times 10^3\ s^{-1}$, also for low substrate concentrations, (s) ≈ 0 (eq A20). It should be noted, however, that the lack of a signal associated with the first exponential speaks against this possibility in conjunction with Model II.

The limit value of α for (s) = 0 is (from eq A19)

$$\alpha_0 = k_{+1}k_{+3}K_iK_m/(k_{+3}K_i + k_{+1}K_m) \qquad \text{(II.5)}$$

where all constants are defined above in eqs II.1−II.4. And that of β, also for (s) = 0 (eq A20), is

$$\beta_0 = k_3K_i + k_{+1}K_m - \alpha_0 \qquad \text{(II.6)}$$

where it is known that $\beta_0 > 5 \times 10^3\ s^{-1}$. The limit value of α for (s) $\rightarrow \infty$ is

$$\alpha_\infty = k_{+1}k_{+3}(K_i + K_m)/(k_{+1} + k_{+3}) \qquad \text{(II.7)}$$

Equation A19 is the sum of a hyperbolic function of the substrate concentration, (s) (Michaelis-type of equation), and an inverse function of (s), which adds a small term ($<\alpha_0$) that disappears as the concentration of the substrate is increased:

$$\alpha = [k_{+1}k_{+3}(K_i + K_m)/(k_{+1} + k_{+3})](s)/[(s) + K_{1,obs}] + [k_{+1}k_{+3}/(k_{+1} + k_{+3})]K_iK_m/[(s) + K_{1,obs}] \qquad \text{(II.8)}$$

$$= [\alpha_\infty/[1 + K_{1,obs}/(s)]] + [\alpha_0K_{1,obs}/[(s) + K_{1,obs}]]$$

where

$$K_{1,obs} = (k_{+3}K_i + k_{+1}K_m)/(k_{+1} + k_{+3}) \qquad \text{(II.9)}$$

With $K_{m,app}$ as defined in eq II.4, note that

$$\alpha_0K_{1,obs}/\alpha_\infty = K_{m,app} \qquad \text{(II.10)}$$

Equation II.8 is thus rather similar to eq I.3, essentially a hyperbolic saturation function of the Michaelis-type with a characteristic substrate concentration, (s) = $K_{1,obs}$, at which α, the observed rate constant, attains the value $^1/_2(\alpha_0 + \alpha_\infty)$. Values of the parameters α_0, α_∞, and $K_{1,obs}$ relating to Model II may be obtained from fitting eq II.8 to the k_{obs} results.

Table 4 shows some of these Model II parameter values resulting from an analysis of the data obtained on the wild-type enzyme. However, it is important to evaluate the "physical" meaning of the results, and this requires some further considerations:

First note that here the experimental error is of the order 3%, and thus within experimental error the sum of two quantities is equal to the larger of these when the smaller is less than 3% of the larger. Thus in the following, "≪" means "less than 3% of".

When the measured quantities $K_{1,obs} \gg K_{m,app}$, we get from eqs II.4 and II.9

$$K_iK_m/(K_i + K_m) = K_{m,app} \ll K_{1,obs} < K_i + K_m \qquad \text{(II.11)}$$

where requires that either $K_i \ll K_m$ or $K_m \ll K_i$.

The latter result actually means that non-productive binding does not occur, since the possibility $K_m \ll K_i$ would lead to $K_{m,app} = K_m$. In this case K_i would have no influence on the steady state kinetic parameters, which is inconsistent with the essential features of Model II. Therefore we shall consider the other possibility, $K_i \ll K_m$. In this condition (eqs II.4 and II.9),

$$K_{m,app} = K_i \quad \text{and } K_{1,obs} \leq K_m \tag{II.12}$$

Furthermore since $\alpha_0 \ll \alpha_\infty < \beta_0$ and $\alpha_0 < K_{+3}K_i$ as well as $\alpha_0 < k_{+1}K_m$, we get

$$k_{+1}k_{+3}K_iK_m/(k_{+3}K_i + k_{+1}K_m) = \alpha_0 \ll 5 \times 10^3\ s^{-1} < \beta_0 = k_{+3}K_i + k_{+1}K_m - \alpha_0 \tag{II.13}$$

It is then required either that:

$$k_{+3}K_i \ll k_{+1}K_m \tag{II.14}$$

leading to $k_{+1}K_m = \beta_0 \geq 5 \times 10^3\ s^{-1}$ and $k_{+3}K_i = \alpha_0$, or that

$$k_{+1}K_m \ll k_{+3}K_i \tag{II.15}$$

leading to $k_{+3}K_i = \beta_0 \geq 5 \times 10^3\ s^{-1}$ and $k_{+1}K_m = \alpha_0$, where II.15 is obviously false, since from II.7 and $K_i \ll K_m$

$$\alpha_\infty = k_{+1}k_{+3}(K_i + K_m)/(k_{+1} + k_{+3}) < 1.03k_{+1}K_m/(1 + k_{+1}/k_{+3}) < 1.03k_{+1}K_m$$

and at the same time it is required that

$$k_{+1}K_m = \alpha_0 \ll \alpha_\infty$$

Thus the result is II.14.

From II.12 and II.14 K_i and k_{+3} are known, and we need to obtain k_{+1} and K_m. It can be shown that $k_{+1} > k_{+3}$, since if we assume $k_{+1} \leq k_{+3}$, we get from eq II.7

$$\alpha_\infty = k_{+1}k_{+3}K_m/(k_{+1} + k_{+3}) \rightarrow k_{+3}K_m \geq k_{+1}K_m \geq \alpha_\infty \geq {}^1/_2k_{+3}K_m \geq {}^1/_2k_{+1}K_m$$

so that the requirement that α_∞ is a measurable quantity at the same time as $\beta_0 = k_{+1}K_m$ is too large to be measured is not fulfilled.

Thus $k_{+1} > k_{+3}$, so that from II.9

$$K_{1,obs} = k_{+1}K_m/(k_{+1} + k_{+3}) \rightarrow 2K_{1,obs} > K_m \geq K_{1,obs} \tag{II.16}$$

and from II.7

$$\alpha_\infty = k_{+1}k_{+3}K_m/(k_{+1} + k_{+3}) \rightarrow k_{+1}K_m > \alpha_\infty \geq k_{+3}K_m \tag{II.17}$$

where the equalities are true if $k_{+3} \ll k_{+1}$.

Within this narrow limit of K_m (II.16) it is now possible to calculate the allowed range of the k_{+2} value, the intrinsic catalytic consant of Model II, which according to the model is *identical* of all the substrates. From eq II.3

$$k_{+2} = k_{cat}(K_i + K_m)/K_i = k_{cat}(K_{m,app} + aK_{1,obs})/K_{m,app} \tag{II.18}$$

where a (II.18) is a limited quantity $1 < a < 2$, as is seen from II.16.

The results of an analysis according to Model II of the experimental kinetic data for the wild-type glucoamylase thus can include the k_{+2} values as shown in Table 4. It is seen that the results on k_{+2} are inconsistent with the essential assumption of Model II, that k_{+2}, the intrinsic catalytic constant, is the same for all substrates.

Conclusions of the Kinetic Analysis. The results of this analysis thus are that Model I, but not Model II, is consistent with the stopped-flow measurements on glucoamylase-catalyzed reactions. Therefore also the usual assignments of subsite interaction energies and arguments based on such subsite interaction energies are seriously questioned. We base the following on Model I (Tables 1−3).

The steady state kinetic results (Tables 1−3) show weak overall binding (K_m and K_d) but effective catalysis (k_c) of the Glu180→Gln mutant; normal or close to wild-type binding (Tables 1−3) but inefficient catalysis of the Asp176→Asn mutant (Sierks et al., 1990). The presteady state results, of which K_1 relates to the first complex formed, ES, and K_2 to the equilibrium of ES and E*S with k_2 as the rate constant of the forward reaction and k_{-2} as the rate constant of the reverse reaction, reveals more details. In general the mutations investigated show insignificant changes in the K_1 value. The only exception is binding of maltose to the Glu180→Gln mutant. As seen from X-ray crystallographic studies (Aleshin et al., 1994; Stoffer et al., 1995) (illustrated in Figure 1) and steady state kinetic studies (Sierks & Svensson, 1992) Glu180 is expected to share a hydrogen bond with the 2-OH of the glucose residue in subsite 2 in the Michaelis complex and/or the transition state complex. According to the lack of effect on K_1 of the Glu180 mutation (Tables 2 and 3), this bond apparently is not established in the first association complex, except perhaps with maltose (Table 1). Non-identity of maltose and of longer substrates with respect to the spatial arrangements and interactions of the second glucose residue of the association complex is indicated.

The second reaction step apparently needs Glu180 as a catalyst of the E*S complex formation, as the k_2 values (Tables 1−3) are strongly affected by the mutation. Glu180 thus assists in the formation of the correct conformation of the Michaelis complex. It seems plausible that the hdyrogen bond to 2-OH of the second glucose residue is established in the transition state of the ES ⇄ E*S reaction step and is important in stabilizing the E*S complex. Mutation of Glu180 results in a slow conformational change (k_2) and a displacement of the equilibrium toward ES; not only does k_2 decrease, but k_{-2} also increases ($K_2 = k_{-2}/k_2$). The loss in binding energy in this step is approximately 8 kJ/mol compared with the wild-type enzyme. This may result from a single hydrogen bond and takes care of most of the overall effects observed in steady state (Sierks & Svensson, 1992). Since the catalytic rate is not or only slightly affected (k_c), the hydrogen bond of Glu180 does not assist in the rate-determining catalytic step. All events after the actual bond

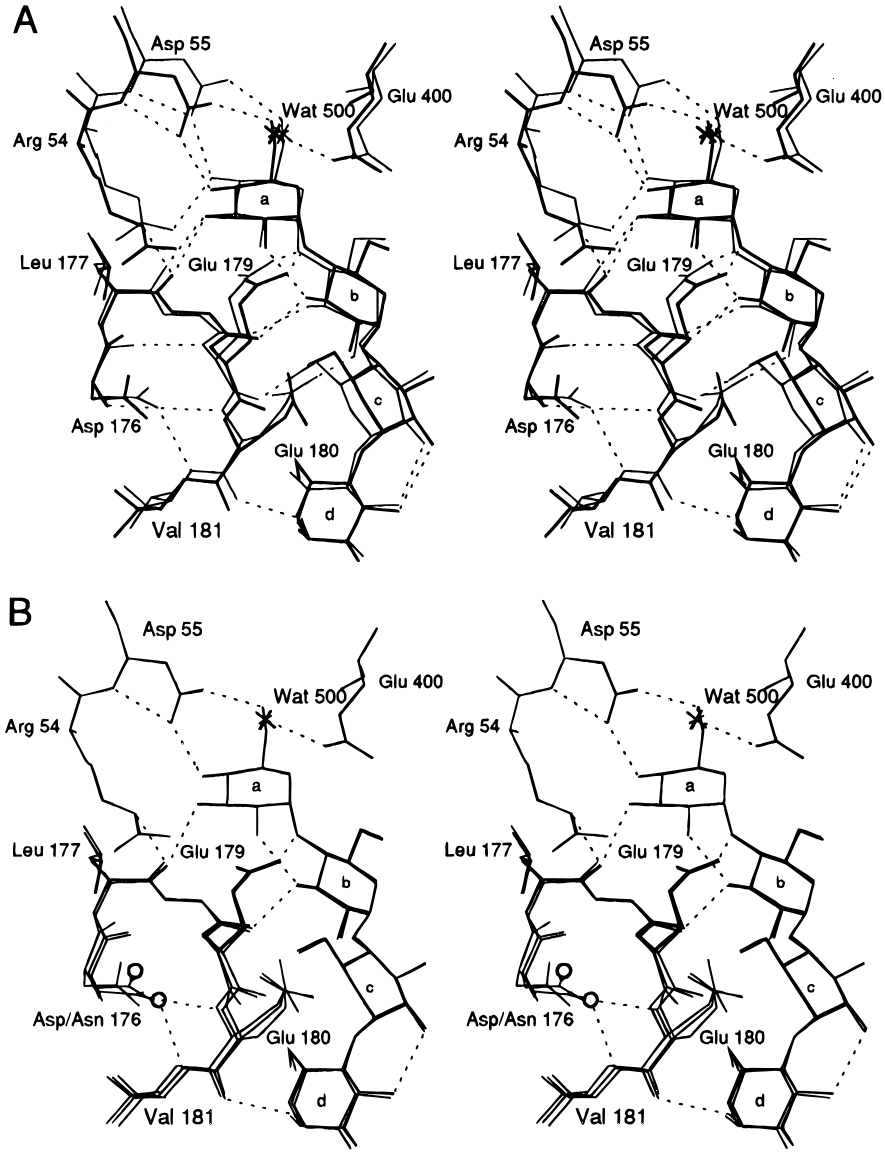

FIGURE 4: Structure models of the active site of glucoamylase from *A. awamori* var. *X100* with maltotetraose. Hydrogen bonds less than 3.0 Å are represented by dashed lines. (A) Wild-type before (solid lines) and after (bold lines) energy minimization. (B) Wild-type and the two conformations of the Asp176→Asn mutant after energy minimizations. The OD1 atoms of each of the Asn176 forms are indicated by circles.

breakage in the substrate are, as seen from the equal values of K_m and K_d (Tables 1−3), faster than (and thus hidden in) the catalytic step. No accumulation of enzyme−product complexes occurs.

Structure Energy Minimization Calculations. Figure 4A shows structure models of the active site of the wild-type glucoamylase from *A. awamori* var. *X100* with maltotetraose before and after minimization calculations. The only apparent differences seen are small changes of the positions of the carboxylate functions of Glu180 and of Asp176. This is in accordance with a dynamic role of Glu180 in the course of the catalytic reaction, as is deduced from the kinetics.

The Asp176→Asn mutant shows no significant kinetic changes of its substrate binding (Tables 1−3). As is illustrated in Figure 1, Asp176 interacts in a hydrogen-bonding network involving also the backbone of the general acid catalyst, Glu179, a region of the active site, which thus does not seem to need adjustments when the substrates bind. But as seen from the large negative effect on k_c (Sierks et al., 1990) in the absence of the carboxylate function of Asp176, this residue is involved in the changes that occur in the rate-determining step, which is assumed to be the transfer of H^+ from Glu179 to the substrate. Adjustments in the hydrogen bond nework involving the backbone of Glu179 thus may play a role in obtaining the transition state geometry. This expected change of the conformation of the β-turn in the Asp176→Asn mutant due to changes in the hydrogen bonds involving Asp176, was further expected to change the ϕ,ψ angles of Glu179 and thus result in the poor catalytic activity of this mutant. But, as is seen from Figure 4B, structural energy minimization calculations on the Asn176 mutant resulted in only minor changes in these angles, and no obvious differences are seen between the position of the carboxylate of Glu179 in the wild-type and the mutant before or after minimization.

DISCUSSION

General Reaction Model of Glucoamylase-Catalyzed Reactions. The kinetics of the hydrolysis of a series of oligomer substrates catalyzed by the wild-type and mutants of glu-

coamylase from *A. niger* has been studied using stopped-flow fluorescence measurements. The results show concentration dependencies of the observed rates and changes of fluorescence intensities of these processes (Tables 1−3) that are in accordance with a three-step reaction model (Model I) in which initial fast association of the substrate is followed by a conformational change of the enzyme−substrate complex in a rather fast step, but with measurable rate, to form the Michaelis complex, the transformation of which is the rate-determining step of the reaction governed by k_c. We have also evaluated the results according to Model II, which is, more or less implicitly, used in calculations of subsite energies of glucoamylase−substrate interactions at subsites 1 and 2. Model II is a classical reaction model that assumes non-productive binding of the substrates and equal intrinsic k_c values (k_{+2}) of all substrates. It is found (Table 4) that the intrinsic k_c values obtained from the stopped-flow measurements and the equations describing Model II are not constant, but vary significantly, actually up to a factor of 10 between maltose and maltotetraose hydrolysis catalyzed by the wild-type glucoamylase. Our results clearly reject Model II.

It seems appropriate to reevlauate conclusions obtained from calculations based on Model II. Ohnishi (1990) attempted to do so and found similar subsite 1 and 2 binding energies, but the calculations were based on the assumption that K_i of glucose could be taken as representative of the subsite 2 interaction energy, since "glucose is bound at subsite 2 of which affinity A_2 is the largest". This may not be correct. Subsite 1 interactions are probably much more important than has hitherto been anticipated. As seen from the 3D structures of stable glucoamylase−inhibitor complexes (Harris et al., 1993; Aleshin et al., 1994; Stoffer et al., 1995) the main interactions of the complexes are due to hydrophobic stacking and hydrogen bonding in subsites 1 and 2, where the sugar ring at subsite 2 participates in three hydrogen bonds with enzymic groups, one of which is the carboxylate of Glu180 (Figure 1), whereas the sugar ring of subsite 1 participates in seven hydrogen bonds. Of other interactions, the most important seems to be stacking of the sugar ring of subsite 3 with Trp120, a residue which also forms a hydrogen bond with the catalytic general acid, Glu179 (Aleshin et al., 1994). Very small, if any, differences in the geometry of the active site has been observed between the free enzyme and the enzyme−inhibitor complexes (Harris et al., 1993; Aleshin et al., 1994; Stoffer et al., 1995). The kinetics, however, reveal conformational changes in the course of the reaction. These may stem from relatively minor adjustments involving several residues and are not necessarily due to the formation or dissociation of particular bonds. Furthermore the change of one residue may affect several others, and additive results of the effects observed on various mutants cannot be expected. Nevertheless, the reaction kinetics (Tables 1−3) indicate an importance of subsite 1 interactions early in the binding process; $K_2 = k_{-2}/k_2$ vlaues are never so small that it seems reasonable to assume that the second step involves the formation of all of the seven hydrogen bonds expected in the Michaelis complex, as is required if the association complex does not involve subsite 1. In all cases, further, the presteady state "equilibrium" constant, K_d, of the substrate binding leads to values equal to K_m, so that steady state concentrations of enzyme−product complexes must be negligibly small. If subsite 2 binding was dominating, accumulation of such complexes would be expected in contrast to what is actually observed.

In conclusion, Model I represents a good working model of glucoamylase-catalyzed reactions, provided that the first association complex, ES, is taken to be one in which the substrate interacts at subsite 1 of the enzyme.

Roles of Glu180 and Asp176 of Glucoamylase. In the crystal structure of the complex between D-*gluco*-dihydroacarbose and glucoamylase from *A. awamori* var. *X100* (Stoffer et al., 1995, Asp176, Leu177, Trp178, and Glu179 are involved in formation of a β-turn which is stabilized by a hydrogen bond of 2.84 Å between the backbone carbonyl of Asp176 and the backbone nitrogen of Glu179, the general catalytic acid. Furthermore, the role of Asp176 as a stabilizing factor for the β-turn is enhanced by two hydrogen bonds of 2.82 and 2.83 Å between Asp176 OD2 and the backbone nitrogens of Glu180 and Val181, respectively. The influence of Asp176 on the activity of glucoamylase is performed indirectly through this β-turn which contains several amino acids that are of outermost importance for binding and hydrolysis of substrates. Leu177, Trp178, and Glu180 are involved in stabilization and binding of substrates or inhibitors by hydrogen bond formation, whereas Glu179 is responsible for hydrogen donation to the glucosidic oxygen of the scissile bond (Figure 1). In addition, the ϕ and ψ angles (62°, 33°) of Glu179 are unusual since they fall in the region for right-handed helices, which indicates that the Glu179 is positioned in a delicate conformation to perform its role as the catalytic acid. The kinetic effects of the Glu180→Gln mutation indicate that the conversion of the association complex, ES, to the Michaelis complex, E*S, involves the formation of the hydrogen bond between Glu180 and the 2-OH of sugar ring 2 and that the interaction of Glu180 at subsite 2 is not established in the association complex, except perhaps for maltose. In the binding process some flexibility of Glu180 is thus required. As seen from the structural energy minimization calculations illustrated in Figure 4, this flexibility is actually found. In energetic terms (Tables 2 and 3), the interaction energy in the Michaelis complex is increased by approximately 9 kJ/mol (7, 9, and 11 kJ/mol of maltose, maltotriose, and maltotetraose, respectively) in the wild-type, and only by 1.7 kJ/mol (all) in the mutant, compared with that of the association complex. This is compatible with the formation of one hydrogen bond in the wild type, which is not formed in the mutant. It seems plausible from these data to suggest that almost full contact is achieved in subsite 1 in the association complex and that most of the additional binding energy of the Michaelis complex stems from the formation of a hydrogen bond from Glu180 to 2-OH of the sugar ring in subsite 2.

The Asp176→Asn mutant primarily shows loss of catalytic efficiency and practically no changes in the actual substrate binding. Its position in the structure in the Asp176−Val181 loop (Figure 1) leads to an expectation of a particular role of Asp176 in keeping the catalytic acid Glu179 in optimal position for catalysis. The results of structural energy minimization calculations (Figure 4B), however, do not support this expectation, since no major differences are immediately seen in the conformation of Glu179 in the wild-type as compared to the mutant. With no structure available of the Asp176→Asn mutant, one may speculate that the folding of the mutant results in another conformation of the

Asn176−Val181 loop giving rise to a changed position of the carboxylate of Glu179.

In summary the results of analysis of the kinetic data obtained in the present study support Model I but contradict Model II. An important implication of this is that allocations of subsite 1 and subsite 2 binding energies, as they are usually made and given in the literature, are based on invalid assumptions and must be seriously questioned. It is our conclusion that calculations of separate subsite 1 and 2 energies are not reliable, even if, as have been done by Ohnishi (1990), they are based on Model I but under the assumptions that the ES complex contains an empty subsite 1 and that glucose binds at subsite 2 with an affinity representing that of a substrate glucose ring.

ACKNOWLEDGMENT

We are grateful to Dorthe Boelskifte and to Sidsel Ehlers for help with mutant enzyme preparation and to Dr. Jan Lehmbeck (Novo Nordisk A/S) for construction and expression of mutant genes.

APPENDIX

Presteady State Kinetic Theory of Model II, a Reaction Model Involving One Enzyme−Substrate, ES, Complex and One Enzyme−Inhibitor, EI, Complex

From the law of mass action

$$e_0 = e + es + ei, \quad \text{so that} \quad e = e_0 - ei - es \tag{A1}$$

where the lower-case letters designate the concentration of the corresponding species and e_0 the total concentration of enzyme.

According to our reaction model, now

$$d(es)/dt = k_{+1}(e)(s) - (k_{-1} + k_{+2})(es) = -(k_{-1} + k_{+2} + k_{+1}(s))(es) + k_{+1}(s)(e_0) - k_{+1}(s)(ei) \tag{A2}$$

$$d(ei)/dt = k_{+3}(e)(i) - k_{-3}(ei) = -(k_{-3} + k_{+3}(i))(ei) + k_{+3}(i)(e_0) - k_{+3}(i)(es) \tag{A3}$$

Isolating (ei) from eq A2 leads to

$$(ei) = -((k_{-1} + k_2)/k_{+1}(s) + 1)(es) + (e_0) - (1/(k_{+1}(s))d(es)/dt) \tag{A4}$$

which when inserted into eq A3 leads to

$$d(ei)/dt = (k_{-3} + k_{+3}(i))[(k_{-1} + k_{+2})/(s) + 1)(es) - (e_0) + (1/(k_{+1}(s))d(es)/dt)] + k_{+3}(i)(e_0) - k_{+3}(i)(es)$$

$$= [(k_{-3} + k_{+3}(i))(K_m/(s)) + k_{-3}](es) - k_{-3}(e_0) + [(k_{-3} + k_{+3}(i))/k_{+1}(s)]d(es)/dt \tag{A5}$$

Differentiation of eq A2 leads to

$$d^2(es)/dt^2 = -(k_{-1} + k_{+2} + k_{+1}(s))d(es)/dt - k_{+1}(s)d(ei)/dt \tag{A6}$$

and when the expression of d(ei)/dt from eq A5 is used, we get after some rearrangements

$$d^2(es)/dt^2 = -[k_{-3} + k_{+3}(i) + k_{+1}(s) + k_{-1} + k_{+2}]d(es)/dt - [k_{-3}(k_{-1} + k_{+2} + k_{+1}(s)) + k_{+3}(i)(k_{-1} + k_{+2})](es) + [k_{-3}k_{+1}(s)](e_0) \tag{A7}$$

which is a second-order differential equation expressing the time dependence of (es).

When we look at only the presteady state phase of the reaction, it is valid to assume that the substrate concentration is not changing if the condition (s) $\gg e_0$ is fulfilled. Here we are further interested in a system in which substrate and inhibitor are identical substances, so that at any time (s) = (i) (constant).

The solution of eq A7 is

$$(es) = (1 - a\exp(-\alpha t) - b\exp(-\beta t))[(e_0)/(1 + K_m/K_i + K_m/(s))] \tag{A8}$$

where $a + b = 1$ and fulfills the limit condition at zero time, (es) = 0, and the term $(1 + K_m/K_i + K_m/(s))$ arises from the steady state concentration of (es) obtained when $t \gg \alpha^{-1}$, defining α as the slower of the rate constants $\alpha < \beta$. Further, α and β are the solutions to the second-order polynomial $Ax^2 - Bx + C$, where A, B, and C are from eq A7 as follows:

$$A = [1/k_{-3}k_{+1}(s)(e_0)] \tag{A9}$$

$$B = [k_{-3} + k_{+3}(i) + k_{+1}(s) + k_{-1} + k_{+2}]/[k_{-3}k_{+1}(s)(e_0)] \tag{A10}$$

$$C = [k_{-3}(k_{-1} + k_{+2} + k_{+1}(s)) + k_{+3}(i)(k_{-1} + k_{+2})]/[k_{-3}k_{+1}(s)(e_0)] \tag{A11}$$

and thus

$$\left.\begin{matrix}\beta\\ \alpha\end{matrix}\right\} = B/2A[1 \pm (1 - (4AC/B^2))^{1/2}] \tag{A12}$$

where, as defined, the minus sign belongs to α ($\alpha < \beta$).

Now $4AC/B^2$ of eq A12 (eqs A9, A10, and A11) becomes

$$4[k_{-3}(k_{-1} + k_{+2} + k_{+1}(s)) + k_{+3}(i)(k_{-1} + k_{+2})]/[k_{-3} + k_{+3}(i) + k_{+1}(s) + k_{-1} + k_{+2}]^2 \tag{A13}$$

which is always smaller than 1, and the approximation

$$(1 - (4AC/B^2))^{1/2} = 1 - 2AC/B^2 \tag{A14}$$

may be allowed. If the two complexes are different, so that K_i and K_m, as well as k_{+1} and k_{+3}, are not (almost) identical, this assumption will hold, and this is implicit in the model: we assume that the two complexes are different. Thus from eq A12:

$$\alpha = (B/2A)(2AC/B^2) = C/B \tag{A15}$$

and

$$\beta = (B/2A)(2 - 2AC/B^2) = B/A - C/B \tag{A16}$$

From eqs A9−A11 and A15, we get

$$\alpha = [k_{-3}(k_{-1} + k_{+2} + k_{+1}(s)) + k_{+3}(i)(k_{-1} + k_{+2})]/[k_{-3} + k_{+3}(i) + k_{+1}(s) + k_{-1} + k_{+2}] \quad \text{(A17)}$$

$$= k_{+1}k_{+3}[K_i(K_m + (s)) + (i)K_m]/[k_{+3}(K_i + (i)) + k_{+1}((s) + K_m)] \quad \text{(A18)}$$

which for (i) = (s) becomes

$$\alpha = k_{+1}k_{+3}[K_iK_m + (K_i + K_m)(s)]/[(k_{+3} + k_{+1})(s) + k_{+3}K_i + k_{+1}K_m] \quad \text{(A19)}$$

From eqs A9−A11 and A16, we now obtain

$$\beta = [k_{-3} + k_{+3}(i) + k_{+1}(s) + k_{-1} + k_{+2}] - \alpha = k_{+3}K_i + k_{+1}K_m + (s)(k_{+1} + k_{+3}) - \alpha \quad \text{(A20)}$$

Note that eqs A19 and A20 are symmetrical with respect to k_{+1} and k_{+3} and to K_m and K_i.

REFERENCES

Aleshin, A., Golubev, A., Firsov, L. M., & Honzatko, R. B. (1992) *J. Biol. Chem. 267*, 19291−19298.

Aleshin, A., Firsov, L. M., & Honzatko, R. B. (1994) *J. Biol. Chem. 269*, 15631−15639.

Clarke, A. J., & Svensson, B. (1984a) *Carlsberg Res. Commun. 49*, 111−122.

Clarke, A. J., & Svensson, B. (1984b) *Carlsberg Res. Commun. 49*, 559−566.

Fagerström, R. (1991) *J. Gen. Microbiol. 137*, 1001−1008.

Fleming, I. D., & Pegler, H. F. (1963) *Analyst 88*, 167−169.

Frandsen, T. P., Dupont, C., Lehmbeck, J., Stoffer, B., Sierks, M. R., Honzatko, R. B., & Svensson, B. (1994) *Biochemistry 33*, 13808−13816.

Frandsen, T. P., Christensen, T., Stoffer, B., Dupont, C., Lehmbeck, J., Honzatko, R. B., & Svensson, B. (1995) *Biochemistry 34*, 10162−10169.

Harris, E. M. S., Aleshin, A. E., Firsov, L. M., & Honzatko, R. B. (1993) *Biochemistry 32*, 1618−1626.

Hiromi, K. (1970) *Biochem. Biophys. Res. Commun. 40*, 1−6.

Hiromi, K. (1995) in *Enzyme Chemistry and Molecular Biology of Amylases and Related Enzymes* (Yamamoto, T., Ed.) CRC Press Inc., Boca Raton, FL.

Hiromi, K., Takahashi, K., Hamauzu, Z., & Ono, S. (1966a) *J. Biochem. (Tokyo) 59*, 469−475.

Hiromi, K., Kawai, M., & Ono, S. (1966b) *J. Biochem. (Tokyo) 59*, 476−480.

Hiromi, K., Nitta, Y., Numata, C., & Ono, S. (1973) *Biochim. Biophys. Acta 302*, 362−375.

Hiromi, K., Ohnishi, M., & Tanaka, A. (1983) *Mol. Cell. Biochem. 51*, 79−95.

Meagher, M. M., Nikolov, Z. L., & Reilly, P. J. (1989) *Biotechnol. Bioeng. 34*, 681−688.

Ohnishi, M. (1990) *Stärke 42*, 311−313.

Ohnishi, M., & Hiromi, K. (1978) *Carbohydr. Res. 61*, 335−341.

Ohnishi, M., Matsumoto, T., Yamanaka, T., & Hiromi, K. (1990) *Carbohydr. Res. 204*, 187−196.

Olsen, K., Svensson, B., & Christensen, U. (1992) *Eur. J. Biochem. 209*, 777−784.

Olsen, K., Christensen, U., Sierks, M. R., & Svensson, B. (1993) *Biochemistry 32* 9686−9693.

Sierks, M. R., & Svensson, B. (1992) *Protein Eng. 5*, 185−188.

Sierks, M. R., & Svensson, B. (1993) *Biochemistry 32*, 1113−1117.

Sierks, M. R., Ford, C., Reilly, P. J., & Svensson, B. (1989) *Protein Eng. 2*, 621−625.

Sierks, M. R., Ford, C., Reilly, P. J., & Svensson, B. (1990) *Protein Eng. 3*, 193−198.

Sierks, M. R., Ford, C., Reilly, P. J., & Svensson, B. (1993) *Protein Eng. 6*, 75−79.

Stoffer, B., Frandsen, T. P., Busk, P. K., Schneider, P., Svendsen, I., & Svensson, B. (1993) *Biochem. J. 292*, 197−202.

Stoffer, B., Aleshin, A. E., Firsov, L. M., Svensson, B., & Honzatko, R. B. (1995) *FEBS Lett. 358*, 57−61.

Svensson, B., & Sierks, M. R. (1992) *Carbohydr. Res. 227*, 29−44.

Svensson, B., & Søgaard, M. (1993) *J. Biotechnol. 29*, 1−37.

Svensson, B., Clarke, A. J., Svendsen, I., & Møller, M. (1990) *Eur. J. Biochem. 188*, 29−38.

Tanaka, A., Ohnishi, M., & Hiromi, K. (1982) *Biochemistry 21*, 107−113.

BI9608323